Acta Cryst. (1985). C**41**, 16–20

Two Crystalline Modifications of Dibromobis(1,2-diaminoethane)platinum(IV) Bis(1,2-diaminoethane)platinum(II) Tetrakis(perchlorate), $[PtBr_2(C_2H_8N_2)_2][Pt(C_2H_8N_2)_2](ClO_4)_4$

BY H. J. KELLER,* B. MÜLLER AND G. LEDEZMA

Anorganisch-Chemisches Institut der Universität Heidelberg, Im Neuenheimer Feld 270, *D*-6900 *Heidelberg* 1, *Federal Republic of Germany*

AND R. MARTIN

Mineralogisches und Kristallographisches Institut der Universität München, Theresienstrasse 2, 8000 *München, Federal Republic of Germany*

(*Received* 14 *October* 1983; *accepted* 23 *July* 1984)

Abstract. $M_r = 1188{\cdot}19$, Mo $K\alpha$, $\lambda = 0{\cdot}71069$ Å, room temperature. (1): monoclinic, $P2$, $a = 7{\cdot}980$ (2), $b = 10{\cdot}979$ (3), $c = 8{\cdot}560$ (2) Å, $\beta = 109{\cdot}36$ (2)°, $Z = 1$, $V = 707{\cdot}62$ Å^3, $D_x = 2{\cdot}79$ g cm^{-3}, $\mu = 132$ cm^{-1}, $F(000) = 554$, $R = 0{\cdot}077$ for 1914 unique reflections. (2): orthorhombic, $Ic2a$, $a = 9{\cdot}687$ (2), $b = 10{\cdot}914$ (8), $c = 13{\cdot}61$ (2) Å, $Z = 2$, $V = 1438{\cdot}90$ Å^3, $D_x = 2{\cdot}74$ g cm^{-3}, $\mu = 130$ cm^{-1}, $F(000) = 1108$, $R = 0{\cdot}0862$ for 718 unique reflections. Both structures are typical Wolffram's salt analogues (WSA's) with infinite chains of planar $[Pt(en)_2]^{2+}$ complex units bridged by bromines. The ligands and the perchlorate counter ions are three-dimensionally ordered presumably because of the strong hydrogen bridges observed. Diffuse sheets appear together with Bragg reflections for k-odd layers. The monoclinic modification can be converted into the orthorhombic form by Cu $K\alpha$ irradiation.

Introduction. The problems in elucidating X-ray structures of Wolffram's salt analogues (WSA's) have been manifold (Keller, 1982). Diffuse patterns, which make the choice of an unambiguous space group more difficult (Beauchamp, Layek & Theophanides, 1982), twinning (Cannas, Marongiu, Keller, Müller & Martin, 1984) and chiral building blocks (Cannas, Marongiu, Martin & Keller, 1983) are among the difficulties recently discussed in detail. Some of the discrepancies could be resolved by observing the temperature dependence of the 'diffuse patterns' down to 4 K (Cannas, Marongiu, Martin & Keller, 1983; Cannas, Marongiu, Keller, Müller & Martin, 1984). On the basis of these data it was proposed that an anisotropic, thermally activated, 'phonon-like' lattice mode – mainly including the chain halides – is responsible for the diffuse patterns. Additional evidence for this 'bromide' lattice mode in WSA has been obtained from resonance Raman data (see, for example, Clark, Kurmoo, Keller, Keppler & Traeger, 1980). More information concerning these problems could be expected from results on very closely related systems. We chose $[Pt(en)_2Br_2][Pt(en)_2](ClO_4)_4$ because it is the first known WSA which exists in two different modifications (Endres, Keller, Martin, Traeger & Novotny, 1980; Bekaroglu, Breer, Endres, Keller & Nam Gung, 1977). The preparation of $[Pt(en)_2Br_2][Pt(en)_2](ClO_4)_4$ primarily leads to the monoclinic phase (1) which is irreversibly converted into the orthorhombic phase (2) by X-ray irradiation (Cu $K\alpha$). Mo $K\alpha$ irradiation destroys most of the crystals, resulting in broad reflection profiles (mosaic spread). In one of the samples we found some crystals which were not as sensitive to X-ray irradiation as most of the other specimens which underwent a phase transition during preliminiary Weissenberg work. We were able to collect diffractometer data of these crystals and herewith report the structure of this solid. In order to clarify the structural relations between the two modifications we re-evaluated the structure of the orthorhombic form including the contributions of the k-odd layer lines.

Experimental. A green crystal of monoclinic (1) obtained as described (Bekaroglu, Breer, Endres, Keller & Nam Gung, 1977), was mounted along the needle axis and characterized by rotating-crystal and Weissenberg photographs (Cu $K\alpha$ radiation). Both methods revealed diffuse scattering patterns in addition to the Bragg reflections for the k-odd layers.

In order to clarify the diffuse pattern a crystal was mounted on a low-temperature X-ray Weissenberg goniometer (Martin, Adlhart & Huber, 1983; Adlhart & Huber, 1982). From 11 to 340 K a series of rotation photographs around the b (needle) axis were taken using Cu $K\alpha_1$ radiation (60 kV rotating anode) focused on the crystal. With an exposure time of 12 h strong

* To whom correspondence should be addressed.

0108-2701/85/010016-05$01.50

Table 1. *Experimental details*

	(1)	(2)
Data collection	$\theta/2\theta$	$\theta/2\theta$
$2\theta_{max}$ (°)	60	60
Range of measured *hkl*	0,0,−11 to 12,6,−3	0,0,4 to 1,15,0
Standard reflections	020, $10\bar{2}$	$10\bar{3}$, $6\bar{2}4$
at intervals	200	100
intensity variation	±0·021, ±0·028	±0·018, ±0·044
Observed reflections $\|I > 0\|$	2144	720
Unique reflections	1914	718
Merging R	0·023	*
Absorption correction	Yes	No
S	5·246	9·404
$(\Delta/\sigma)_{max}$	7·683†	1·194‡
Max., min. $\Delta\rho$ (e Å^{-3})	7·72, −11·65§	7·25, −5·66¶

* No equivalent reflections.
† Largest shift for oscillating chain Br(2).
‡ Largest shift for disordered O(3*a*) of ClO_4^- ('smeared' peak).
§ Highest peak is located 0·44 Å from Pt(1) along the chain.
¶ Highest peak is located 0·80 Å from Pt(1) along the chain.

modulated diffusions could be observed together with the Bragg reflections for the *k*-odd layers. Starting at 340 K these became continuously weaker as the temperature was lowered. Compared with 340 K the 11 K photograph exhibits the same modulated diffusions but with an overall intensity just above the film background. The behaviour of the Bragg reflections was 'normal'. In particular, no hint of the occurrence of super-reflections was found down to 11 K.

These experimental findings suggest that the diffusions in the *k*-odd layers are caused by a thermally activated movement of the Br^- ions along the chain direction. This anisotropic motion may be described as a 'phonon-like' mode (Cannas, Marongiu, Martin & Keller, 1983; Cannas, Marongiu, Keller, Müller & Martin, 1984), as 'mobile valence-alternation domain walls' (Ichinose, 1984), or by similiar dynamic models. In any case: a Br^--disordered 'time-averaged' picture of the excited states of the crystal is obtained from the X-ray data at room temperature. Because of this we used split Br^- positions with a time-averaged partial occupancy in the later refinements. The twofold-degenerate ground state of the crystal (Ichinose, 1984) with three-dimensionally ordered fixed Br^- positions is only accessible at very low temperatures.

Monoclinic (1). No systematic absences, corresponding to space groups *P*2, *Pm* and *P*2/*m*. Lattice parameters from the setting angles of 25 machine-centered reflections (Syntex *R*3, monochromatic Mo *K*α radiation). For further experimental information see Table 1. Refinement based on *F*, $w = 1/\sigma^2(F)$, 'cascade matrix' on Nova 3 computer using *SHELXTL* (Sheldrick, 1981). Scattering factors from *International Tables for X-ray Crystallography* (1974).

Heavy atoms from Patterson synthesis; difference Fourier maps for C, N and O atoms (H not located). Symmetrically 'split' sites were used for the Br^- ions in their located positions at $y = 0{\cdot}26$ and $y = 0{\cdot}76$. If the site-occupation factor was not fixed, final refinement yielded 30% occupation for $y = 0{\cdot}25$ [Br(1)] and $y = 0{\cdot}77$ [Br(3)] and 70% occupation for $y = 0{\cdot}22$ [Br(2)] and $y = 0{\cdot}73$ [Br(4)]. In our opinion the result of this mathematical fitting process reflects problems with the handling of the data obtained from these rather poor quality crystals. The physical implications of this result would be an unsymmetrical electronic potential between two adjacent Pt sites. In view of the experimental problems these implications are not discussed in detail.

Because it is not necessary in space group *P*2 to place Pt(2) exactly at $y = \frac{1}{2}$ a proof for this model may be obtained by using the 299 *k*-odd reflections only. If both metal ions occupy the sites at $y = 0$ and $\frac{1}{2}$ they do not contribute to these reflections. Therefore, we calculated values for R_m (*i.e.* before least-squares refinement) and obtained 0·39 including Pt(2) and 0·50 without it. This suggests a small contribution from Pt(2), but refinements with y variable resulted only in a negligible shift for Pt(2) ($y = 0{\cdot}5002$). This result finally justifies the choice of Pt(2) fixed at exactly 0·5. The rather high value for R_m may be an effect of measuring the 'pure' *k*-odd reflections together with the diffuse background observed as diffuse layer lines on rotation photographs. The differences between calculated and observed structure factors are found to be largest for the *k*-odd reflections. The calculated structure factors were mostly smaller than the observed ones.

Refinement in space group *P*2 yielded $R_w = 0{\cdot}0725$, $R = 0{\cdot}077$, for 86 refined parameters, including anisotropic temperature factors for six atoms (Pt, Br). To check the correctness of the space group chosen we also refined the structure in *Pm*, resulting in unreasonable values of R_w (0·149, all reflections) and R_m (0·55, *k*-odd reflections) compared with the values obtained in *P*2. In space group *Pm* it is suitable to place the perchlorate ion just on the mirror plane and the Pt exactly at $y = 0{\cdot}25$. In contrast to *P*2 the two metal ions become crystallographically equivalent and consequently the crystal structure which results is quite different from that in *P*2.

Orthorhombic (2). Prepared from $Pt(en)_2Cl_2$ (30 mg, 0·078 mmol) dissolved in 3 ml of cold water containing a few drops of 20% aqueous perchloric acid. Mixture placed in a desiccator together with a diluted aqueous mixture of HBr and bromine. After standing at 277 K for a few days green crystals were collected by filtration. Crystal approximately 0·3 × 0·5 × 0·3 mm mounted along needle axis. Rotating-crystal and Weissenberg photographs showed orthorhombic symmetry, systematic absences *hkl* for $h + k + l = 2n + 1$, *h*0*l* for $h = 2n + 1$ and $l = 2n + 1$ corresponding to space groups *Ic*2*a* and *Icma*. Again, diffuse patterns appeared on the *k*-odd layers, diminishing in intensity on lowering the temperature. These results again justify the use of split Br^- positions in the following refinements. Data collection on a Siemens AED diffractometer,

lattice parameters based on 39 reflections. Mo $K\alpha$ radiation, five-value measurement, $2\theta_{max} = 60°$.

Heavy atoms from Patterson synthesis; following calculations performed in *Ic2a*. Fourier and difference Fourier maps showed peaks for the N and C atoms of the ethanediamine ligand (H not located). Instead of four peaks for the O atoms of the perchlorate six maxima were found corresponding to two different orientations for the molecule in the lattice. Split positions for the two O atoms lying in the same plane with Cl at $y = \frac{1}{4}$ were found. This arrangement agrees with that of the monoclinic phase (1). The position for Br^- in the chain was first located at $y = 0{\cdot}25$ but was shifted to $y = 0{\cdot}217$ in further refinement cycles with an increasing value for temperature factor U_{22}. Assuming thermal motion in the chain direction (see below) we split the position and refined the parameters which were not fixed but correlated to each other. We obtained site-occupation factors of 70% ($y = 0{\cdot}282$) and 30% ($y = 0{\cdot}218$) analogous to the situation in the monoclinic phase (1). Difficulties arose with locating reasonable positions for the C atoms of the chelate ligand. During refinement they were shifted just into the PtN_4 plane. In further refinements these C atoms were readjusted into the fixed positions found with the first refinement cycle.

Final $R_w = 0{\cdot}0828$, $R = 0{\cdot}0861$, for 48 refined parameters including anisotropic temperature factors for four atoms (Pt, Br, Cl). Calculations in the centrosymmetric space group *Icma* resulted in R values of ~0·13. As in (1) the perchlorate ion was placed at the mirror plane and the platinum ion at $0,\frac{1}{4},0$. This confirms our choice of *Ic2a* as the correct space group. With respect to the 100 observed reflections of the k-odd layer lines we obtained $R_m = 0{\cdot}129$ (*Ic2a*) and 0·27 (*Icma*).

Discussion. *Monoclinic* (1). Atomic coordinates are listed in Table 2, bond lengths and angles in Table 3.* The contents of a unit cell are shown in Fig. 1. Complex units of $[Pt(en)_2]$ cations are bridged by Br forming linear chains parallel to **b**. The repeat distance of 10·98 Å in the chain direction comprises two cations. The perchlorate counter ions are placed between the cation strands at $y = \frac{1}{4}$ and $\frac{3}{4}$. The closest distances for N–H···O are 2·59 and 2·84 Å, indicating strong intrachain H bonding. The H bonds possibly cause three-dimensional ordering of ligand atoms (see Table 6 and Fig. 2). Every single complex unit is chiral having the configuration $\delta\delta$ or $\lambda\lambda$. Both enantiomeric forms exist in the structure and are stacked alternately in the chains.

* Lists of structure factors and anisotropic thermal parameters for structures (1) and (2) have been deposited with the British Library Lending Division as Supplementary Publication No. SUP 39657 (26 pp.). Copies may be obtained through The Executive Secretary, International Union of Crystallography, 5 Abbey Square, Chester CH1 2HU, England.

Table 2. *Atom coordinates* ($\times 10^4$) *and temperature factors* ($Å^2 \times 10^3$) *in* (1)

	x	y	z	U
Pt(1)	0	0	0	4 (1)*
Pt(2)	0	5000	0	28 (1)*
Br(1)	0	2673 (13)	0	27 (2)*
Br(2)	0	7327 (13)	0	27 (2)*
Br(3)	0	7749 (7)	0	38 (1)*
Br(4)	0	2251 (7)	0	38 (1)*
Cl(1)	6404 (12)	2569 (19)	2801 (11)	36 (2)
Cl(2)	6822 (11)	7544 (18)	2605 (9)	31 (2)
N(1)	2753 (25)	38 (44)	1231 (26)	11 (4)
N(2)	144 (36)	213 (36)	2330 (34)	21 (7)
N(3)	2683 (31)	5198 (29)	843 (31)	18 (6)
N(4)	−42 (32)	5004 (52)	2486 (30)	15 (5)
C(1)	3218 (28)	206 (23)	2824 (28)	9 (4)
C(2)	1783 (73)	427 (53)	3851 (66)	55 (14)
C(3)	3020 (88)	5379 (64)	3144 (76)	74 (19)
C(4)	1887 (33)	4726 (22)	3470 (33)	9 (5)
O(1)	4489 (34)	2709 (39)	2479 (32)	44 (7)
O(2)	7270 (38)	2308 (32)	4533 (37)	47 (9)
O(3)	7212 (83)	3651 (74)	2209 (79)	123 (23)
O(4)	6832 (43)	1417 (32)	2191 (41)	35 (8)
O(5)	6189 (37)	8574 (33)	1483 (35)	31 (6)
O(6)	5942 (29)	7692 (32)	3874 (26)	32 (5)
O(7)	6608 (36)	6485 (26)	1745 (36)	18 (5)
O(8)	8743 (35)	7412 (47)	3481 (32)	43 (7)

* Equivalent isotropic U defined as one third of the trace of the orthogonalized U_{ij} tensor.

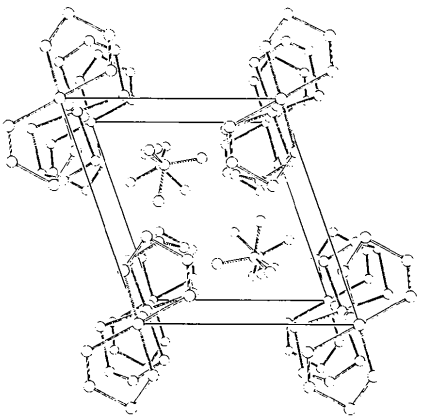

Fig. 1. The unit-cell contents of (1) viewed down the *b* axis.

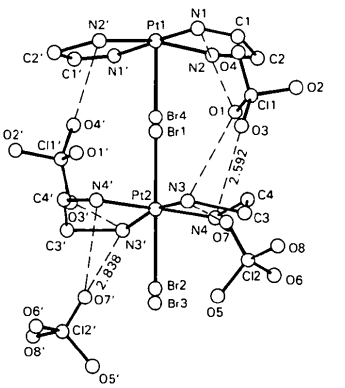

Fig. 2. Segment of a single cation chain in (1) with adjacent perchlorate counter ions. Intrachain N–H···O bridges are indicated by dashed lines; the lengths of the shortest are given in Å.

Table 3. *Bond lengths* (Å) *and angles* (°) *in* (1)

Pt(1)–Br(1)	2·935 (14)	Pt(1)–Br(4)	2·471 (8)
Pt(1)–N(1)	2·098 (16)	Pt(1)–N(2)	1·973 (30)
Pt(1)–Br(2*a*)	2·935 (14)	Pt(1)–Br(3*a*)	2·471 (8)
Pt(1)–N(1*a*)	2·098 (18)	Pt(1)–N(2*a*)	1·973 (30)
Pt(2)–Br(1)	2·555 (14)	Pt(2)–Br(2)	2·555 (14)
Pt(2)–Br(3)	3·019 (8)	Pt(2)–Br(4)	3·019 (8)
Pt(2)–N(3)	2·032 (23)	Pt(2)–N(4)	2·140 (27)
Pt(2)–N(3*a*)	2·032 (23)	Pt(2)–N(4*a*)	2·140 (27)
Br(1)–Br(4)	8·464 (16)	Br(2)–Br(3)	0·464 (16)
Br(2)–Pt(1*a*)	2·935 (14)	Br(3)–Pt(1*a*)	2·471 (8)
Cl(1)–O(1)	1·468 (29)	Cl(1)–O(2)	1·442 (30)
Cl(1)–O(3)	1·517 (81)	Cl(1)–O(4)	1·453 (41)
Cl(2)–O(5)	1·461 (37)	Cl(2)–O(6)	1·485 (28)
Cl(2)–O(7)	1·357 (34)	Cl(2)–O(8)	1·473 (26)
N(1)–C(1)	1·302 (32)	N(2)–C(2)	1·491 (52)
N(3)–C(3)	1·908 (71)	N(4)–C(4)	1·521 (34)
C(1)–C(2)	1·732 (71)	C(3)–C(4)	1·256 (76)
Pt(1*a*)–Br(3)	2·471 (8)	Br(2*a*)–Br(3*a*)	0·464 (16)
Br(3*a*)–Pt(1)	2·471 (8)	Br(3*a*)–Br(2*a*)	0·464 (16)
N(1*a*)–Pt(1)	2·098 (18)	N(2*a*)–Pt(1)	1·973 (38)
N(3*a*)–Pt(2)	2·032 (23)	N(4*a*)–Pt(2)	2·140 (27)
Br(4)–Pt(1)–N(1)	88·9 (13)	Br(1)–Pt(1)–N(1)	88·9 (13)
Br(4)–Pt(1)–N(2)	83·2 (11)	Br(1)–Pt(1)–N(2)	83·2 (11)
Br(1)–Pt(1)–Br(2*a*)	180·0	N(1)–Pt(1)–N(2)	77·8 (10)
N(1)–Pt(1)–Br(2*a*)	91·1 (13)	Br(4)–Pt(1)–Br(2*a*)	180·0
Br(1)–Pt(1)–Br(3*a*)	100·0	N(2)–Pt(1)–Br(2*a*)	96·8 (11)
N(1)–Pt(1)–Br(3*a*)	91·1 (13)	Br(4)–Pt(1)–Br(3*a*)	180·0
Br(4)–Pt(1)–N(1*a*)	88·9 (13)	N(2)–Pt(1)–Br(3*a*)	96·8 (11)
N(2)–Pt(1)–N(1*a*)	101·9 (10)	Br(1)–Pt(1)–N(1*a*)	88·9 (13)
Br(3*a*)–Pt(1)–N(1*a*)	91·1 (13)	N(1)–Pt(1)–N(1*a*)	177·7 (19)
Br(4)–Pt(1)–N(2*a*)	83·2 (11)	Br(2*a*)–Pt(1)–N(1*a*)	91·1 (13)
N(2)–Pt(1)–N(2*a*)	166·4 (23)	Br(1)–Pt(1)–N(2*a*)	83·2 (11)
Br(3*a*)–Pt(1)–N(2*a*)	96·8 (11)	N(1)–Pt(1)–N(2*a*)	101·9 (10)
Br(1)–Pt(2)–Br(2)	180·0	Br(2*a*)–Pt(1)–N(2*a*)	96·8 (11)
Br(2)–Pt(2)–Br(4)	188·0	N(1*a*)–Pt(1)–N(2*a*)	77·8 (10)
Br(1)–Pt(2)–N(3)	96·1 (9)	Br(1)–Pt(2)–Br(3)	180·0
Br(3)–Pt(2)–N(3)	83·9 (9)	Br(3)–Pt(2)–Br(4)	188·0
Br(1)–Pt(2)–N(4)	50·1 (15)	Br(2)–Pt(2)–N(3)	83·9 (9)
Br(3)–Pt(2)–N(4)	89·9 (15)	Br(4)–Pt(2)–N(3)	96·1 (9)
N(3)–Pt(2)–N(4)	50·5 (10)	Br(2)–Pt(2)–N(4)	89·9 (15)
Br(2)–Pt(2)–N(3*a*)	83·9 (9)	Br(4)–Pt(2)–N(4)	90·1 (15)
Br(4)–Pt(2)–N(3*a*)	96·1 (9)	Br(1)–Pt(2)–N(3*a*)	96·1 (9)
N(4)–Pt(2)–N(3*a*)	89·5 (10)	Br(3)–Pt(2)–N(3*a*)	83·9 (9)
Br(2)–Pt(2)–N(4*a*)	89·9 (15)	N(3)–Pt(2)–N(3*a*)	167·7 (18)
Br(4)–Pt(2)–N(4*a*)	80·1 (15)	Br(1)–Pt(2)–N(4*a*)	90·1 (15)
N(4)–Pt(2)–N(4*a*)	179·8 (26)	Br(3)–Pt(2)–N(4*a*)	89·9 (15)
Pt(1)–Br(1)–Pt(2)	180·0	N(3)–Pt(2)–N(4*a*)	89·5 (10)
Pt(2)–Br(1)–Br(4)	180·0	N(3*a*)–Pt(2)–N(4*a*)	90·5 (10)
Pt(2)–Br(2)–Pt(1*a*)	180·0	Pt(2)–Br(2)–Br(3)	180·0
Br(2)–Br(3)–Pt(1*a*)	180·0	Pt(2)–Br(3)–Pt(1*a*)	180·0
Pt(1)–Br(4)–Br(1)	100·0	Pt(1)–Br(4)–Pt(2)	180·0
O(1)–Cl(1)–O(2)	109·2 (19)	O(1)–Cl(1)–O(3)	112·8 (32)
O(2)–Cl(1)–O(3)	112·8 (26)	O(1)–Cl(1)–O(4)	112·2 (23)
O(2)–Cl(1)–O(4)	96·1 (21)	O(3)–Cl(1)–O(4)	112·7 (35)
O(3)–Cl(2)–O(6)	104·6 (20)	O(5)–Cl(2)–O(7)	110·6 (18)
O(6)–Cl(2)–O(7)	119·0 (22)	O(5)–Cl(2)–O(8)	119·1 (24)
O(6)–Cl(2)–O(8)	107·7 (15)	O(7)–Cl(2)–O(8)	96·6 (23)
Pt(1)–N(1)–C(1)	114·6 (18)	Pt(1)–N(2)–C(2)	130·8 (33)
Pt(2)–N(3)–C(3)	98·6 (23)	Pt(2)–N(4)–C(4)	101·8 (19)
N(1)–C(1)–C(2)	123·1 (23)	N(2)–C(2)–C(1)	93·2 (35)
N(3)–C(3)–C(4)	107·8 (38)	N(4)–C(4)–C(3)	115·7 (36)
Pt(1)–Br(3*a*)–Br(2*a*)	180·0		

Table 4. *Atom coordinates* ($\times 10^4$) *and temperature factors* (Å$^2 \times 10^3$) *in* (2)

	x	*y*	*z*	*U*
Pt(1)	0	0	0	25 (1)*
Br(1)	0	−2178 (7)	0	65 (1)*
Br(2)	0	12178 (7)	0	65 (1)*
Cl(1)	791 (13)	2659 (21)	2982 (10)	49 (4)*
N(1)	1505 (70)	168 (64)	−1224 (42)	71 (22)
N(2)	1620 (26)	108 (39)	5754 (20)	8 (5)
C(1)	2815	850	424	50 (9)
C(2)	2917	−228	−539	50 (9)
O(1)	272 (56)	3669 (45)	2781 (37)	62 (16)
O(2)	229 (32)	1526 (42)	2503 (33)	52 (12)
O(3)	1084 (114)	2697 (151)	4009 (68)	91 (14)
O(4)	2083 (89)	2383 (113)	3462 (60)	91 (14)
O(3*a*)	−211 (100)	2676 (94)	−4064 (56)	91 (14)
O(4*a*)	−1927 (85)	2475 (172)	−2156 (62)	91 (14)

* Equivalent isotropic *U* defined as one third of the trace of the orthogonalized U_{ij} tensor.

Orthorhombic (2). Atomic coordinates, bond lengths and angles are listed in Tables 4 and 5. The structure can be described similarly to the monoclinic phase. Fig. 3 shows chains containing [Pt(en)$_2$] cations and Br$^-$ as bridging halide running parallel to **b**. As found in the monoclinic phase the orthorhombic structure also contains both enantiomers. The puckered single complex units are chiral in $\delta\delta$ or $\lambda\lambda$ conformations stacked alternately in the chains. Adjacent chains are H-bonded through interactions with the perchlorate which is placed at $y = \frac{1}{4}$ and $y = \frac{3}{4}$. The distances for N–H···O are longer compared to those found in the monoclinic phase (1), except for one interchain contact (2·81 Å) not found in (1) (see Table 6 and Fig. 4). A slight decrease of the density should be noted.

Both structures are fully three-dimensionally ordered with exception of the chain Br$^-$ and the perchlorate counter ions. While the latter are statistically disordered but fixed 'in time' the Br$^-$ positions reflect a 'time-averaged' description of the lattice.

Table 5. *Bond lengths* (Å) *and bond angles* (°) *in* (2)

Pt(1)–Br(1)	2·377 (8)	Pt(1)–N(1)	2·221 (62)
Pt(1)–N(2)	2·058 (26)	Pt(1)–Br(1*a*)	3·080 (8)
Pt(1)–Br(2*a*)	2·377 (8)	Pt(1)–Br(2*b*)	3·080 (8)
Pt(1)–N(1*a*)	2·221 (62)	Pt(1)–N(2*a*)	2·058 (26)
Br(1)–Pt(1*b*)	3·080 (8)	Br(1)–Br(2*b*)	0·703
Br(2)–Pt(1*a*)	2·377 (8)	Br(2)–Pt(1*c*)	3·080 (8)
Br(2)–Br(1*b*)	0·703	Cl(1)–O(1)	1·242 (55)
Cl(1)–O(2)	1·500 (51)	Cl(1)–C(3)	1·427 (93)
Cl(1)–O(4)	1·444 (88)	Cl(1)–O(3*aa*)	1·577 (80)
Cl(1)–O(4*aa*)	1·586 (90)	N(1)–C(2)	1·711 (66)
N(2)–C(1)	1·599 (31)	C(1)–C(2)	1·763
O(3)–O(4)	1·268 (139)	O(3)–O(3*aa*)	0·850 (148)
O(4)–O(4*aa*)	1·788 (117)	O(3*a*)–Cl(1*a*)	1·577 (80)
O(3*a*)–O(3*a*)	0·850 (148)	O(4*a*)–Cl(1*a*)	1·586 (90)
O(4*a*)–O(4*a*)	1·788 (117)	Pt(1*a*)–Br(1*b*)	3·080 (8)
Pt(1*b*)–Br(2*b*)	2·377 (8)	Pt(1*c*)–Br(2)	3·060 (8)
Pt(1*c*)–Br(1*b*)	2·377 (8)	Br(1*a*)–Br(2*a*)	0·703
Br(1*b*)–Br(2)	0·703	Br(1*b*)–Pt(1*a*)	3·080 (8)
Br(1*b*)–Pt(1*c*)	2·377 (8)	Br(2*a*)–Br(1*a*)	0·703
Br(2*b*)–Pt(1)	3·080 (8)	Br(2*a*)–Br(1)	0·703
Br(2*b*)–Pt(1*b*)	2·377 (8)	Cl(1*a*)–O(3*a*)	1·577 (80)
Cl(1*a*)–O(4*a*)	1·586 (50)	Cl(1*a*)–O(3*a*)	1·427 (93)
Cl(1*a*)–O(4*a*)	1·444 (88)	H(2*a*)–Pt(1)	2·058 (26)
O(3*a*)–O(3*a*)	0·850 (148)	O(3*a*)–Cl(1*a*)	1·427 (93)
O(3*a*)–O(4*a*)	1·268 (139)	O(4*a*)–O(4*a*)	1·788 (117)
O(4*a*)–Cl(1*a*)	1·444 (88)	O(4*a*)–O(3*a*)	1·268 (139)
O(3*aa*)–O(3)	0·850 (148)	O(4*aa*)–O(4)	1·788 (117)
Br(1)–Pt(1)–N(1)	94·7 (18)	Br(1)–Pt(1)–N(2)	93·3 (12)
N(1)–Pt(1)–N(2)	88·8 (18)	Br(1)–Pt(1)–Br(1*a*)	180·0
N(1)–Pt(1)–Br(1*a*)	85·3 (18)	N(2)–Pt(1)–Br(1*a*)	86·7 (12)
Br(1)–Pt(1)–Br(2*a*)	180·0	N(1)–Pt(1)–Br(2*a*)	85·3 (18)
N(2)–Pt(1)–Br(2*a*)	86·7 (12)	N(1)–Pt(1)–Br(2*b*)	94·7 (18)
N(2)–Pt(1)–Br(2*b*)	83·3 (12)	Br(1*a*)–Pt(1)–Br(2*b*)	180·0
Br(2*a*)–Pt(1)–Br(2*b*)	180·0	Br(1)–Pt(1)–N(1*a*)	94·7 (18)
N(1)–Pt(1)–N(1*a*)	170·6 (36)	N(2)–Pt(1)–N(1*a*)	90·7 (18)
Br(1*a*)–Pt(1)–N(1*a*)	85·3 (18)	Br(2*a*)–Pt(1)–N(1*a*)	85·3 (18)
Br(2*b*)–Pt(1)–N(1*a*)	94·7 (18)	Br(1)–Pt(1)–N(2*a*)	93·3 (12)
N(1)–Pt(1)–N(2*a*)	90·7 (18)	N(2)–Pt(1)–N(2*a*)	173·4 (24)
Br(1*a*)–Pt(1)–N(2*a*)	86·7 (12)	Br(2*a*)–Pt(1)–N(2*a*)	86·7 (12)
Br(2*b*)–Pt(1)–N(2*a*)	93·3 (12)	N(1*a*)–Pt(1)–N(2*a*)	88·8 (18)
Pt(1)–Br(1)–Pt(1*b*)	180·0	Pt(1)–Br(1)–Br(2*b*)	180·0
Pt(1*a*)–Br(2)–Br(1*b*)	180·0	Pt(1*a*)–Br(2)–Pt(1*c*)	180·0
O(1)–Cl(1)–O(2)	119·3 (31)	O(1)–Cl(1)–O(3)	105·7 (69)
O(2)–Cl(1)–O(3)	121·5 (68)	O(1)–Cl(1)–O(4)	129·5 (55)
O(2)–Cl(1)–O(4)	109·9 (52)	O(3)–Cl(1)–O(4)	52·4 (58)
O(1)–Cl(1)–O(3*aa*)	92·9 (45)	O(2)–Cl(1)–O(3*aa*)	106·6 (42)
O(3)–Cl(1)–O(3*aa*)	32·4 (57)	O(4)–Cl(1)–O(3*aa*)	83·6 (49)
O(1)–Cl(1)–O(4*aa*)	103·7 (66)	O(2)–Cl(1)–O(4*aa*)	80·8 (60)
O(3)–Cl(1)–O(4*aa*)	124·1 (56)	O(4)–Cl(1)–O(4*aa*)	72·1 (47)
O(3*aa*)–Cl(1)–O(4*aa*)	155·7 (53)	Pt(1)–N(1)–C(2)	95·5 (25)
Pt(1)–N(2)–C(1)	106·2 (15)	N(2)–C(1)–C(2)	92·9 (13)
N(1)–C(2)–C(1)	101·1 (22)	Cl(1)–O(3)–O(4)	64·5 (59)

Table 6. N···O *interatomic distances* [Å, *e.s.d.'s* 0·025 Å *for* (1), 0·07 Å *for* (2)]

'intra' and 'inter' refer to the type of H bonding: intrachain for strong interactions within the same chain, interchain H bridges between adjacent chains. O atoms marked with an asterisk lie below the imaginary plane containing Cl and the remaining O atoms (unmarked).

Monoclinic (1)			Orthorhombic (2)		
O(1)	N(1)	3·268	O(1)*	N(1)	2·925
O(1)	N(3)	3·189	O(1)*	N(2)	3·436
O(3)*	N(3')	3·141	O(2)*	N(1)	2·831 intra
O(3)*	N(4)	2·592 intra	O(2)*	N(2)	2·915
O(4)*	N(1)	3·434	O(4)	N(1)	2·813 inter
O(4)*	N(1')	3·410	O(4)	N(2)	3·323
O(5)*	N(1')	3·161	O(4*a*)	N(1)	3·231
O(5)*	N(1)	3·124	O(4*a*)	N(2)	3·058
O(7)*	N(3)	3·286			
O(7)*	N(3')	2·838 intra			
O(7)*	N(4)	3·011			
O(8)	N(4)	3·034			

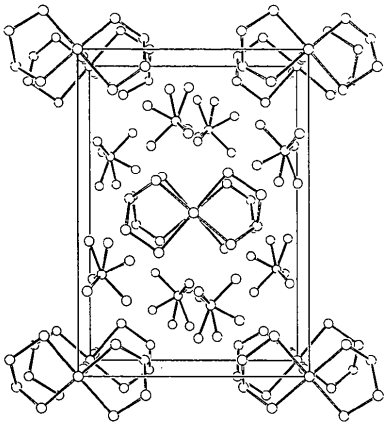

Fig. 3. The unit-cell contents of (2) viewed down the *b* axis.

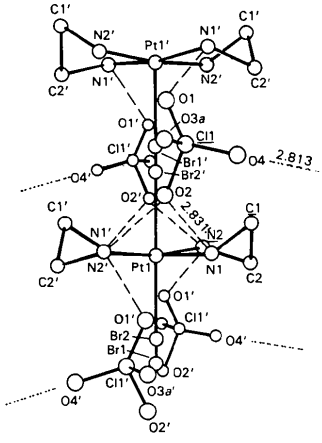

Fig. 4. Segment of a single cation chain in (2) with adjacent perchlorate counter ions. Intrachain N—H···O bridges are indicated by dashed lines, interchain bridges by dotted lines; lengths of the shortest are given in Å.

For the first time we have observed and characterized a phase transition induced by X-ray irradiation in a WSA. The difference between the two phases is most pronounced in the H-bridge pattern: in monoclinic (1) interactions exist within the same chain in contrast to the orthorhombic form (2) where H bonding occurs between adjacent chains. So, the observed phase transition which is accompanied by a slight decrease in density may be regarded as a change in the H-bridging pattern: from an 'intrachain' to an 'interchain' one. The H-bonding pattern is the only remarkable difference between the two forms (1) and (2), other structural details being similar – for example, the 'racemic' build up of the enantiomeric complex molecules in alternating stacks along the chains.

It may be informative to point out the differences between the data of (2) reported here and those found in the X-ray analysis by Breer, Endres, Keller & Martin (1978). We registered systematic absences in $0k0$ for $k = 2n + 1$ not found by Breer *et al.* This causes a change in space group from $I222$ to $Ic2a$. In view of the temperature-dependent data of the 'diffusions' we split Br sites and were able to refine the structure without problems and obtained useful bond lengths, bond angles, *etc.*

This work was supported by the Deutsche Forschungsgemeinschaft, grant No. Ke135/29-2.

References

ADLHART, W. & HUBER, H. (1982). *J. Appl. Cryst.* **15**, 241–244.

BEAUCHAMP, A. L., LAYEK, D. & THEOPHANIDES, T. (1982). *Acta Cryst.* B**38**, 1158–1164, and references cited therein.

BEKAROGLU, Ö., BREER, H., ENDRES, H., KELLER, H. J. & NAM GUNG, H. (1977). *Inorg. Chim. Acta*, **21**, 183–186.

BREER, H., ENDRES, H., KELLER, H. J. & MARTIN, R. (1978). *Acta Cryst.* B**34**, 2295–2297.

CANNAS, M., MARONGIU, G., KELLER, H. J., MÜLLER, B. & MARTIN, R. (1984). *Z. Naturforsch. Teil B*, **39**, 197–200, and references cited therein.

CANNAS, M., MARONGIU, G., MARTIN, R. & KELLER, H. J. (1983). *Z. Naturforsch. Teil B*, **38**, 1346–1350, and references cited therein.

CLARK, R. J. H., KURMOO, M., KELLER, H. J., KEPPLER, B. & TRAEGER, U. (1980). *J. Chem. Soc. Dalton Trans.* pp. 2498–2502.

ENDRES, H., KELLER, H. J., MARTIN, R., TRAEGER, U. & NOVOTNY, M. (1980). *Acta Cryst.* B**36**, 35–39.

ICHINOSE, S. (1984). *Solid State Commun.* **50**, 137–140.

International Tables for X-ray Crystallography (1974). Vol. IV. Birmingham: Kynoch Press.

KELLER, H. J. (1982). *Extended Linear Chain Compounds*, Vol. 1, edited by J. S. MILLER, pp. 357–407. New York: Plenum.

MARTIN, R., ADLHART, W. & HUBER, H. (1983). Private communication.

SHELDRICK, G. M. (1981). *SHELXTL. An Integrated System for Solving, Refining and Displaying Crystal Structures from Diffraction Data.* Univ. Göttingen.